Available online at www.sciencedirect.com
ScienceDirect
Journal of the European Ceramic Society 30 (2010) 2653–2660
www.elsevier.com/locate/jeurceramsoc

High temperature oxidation of SiC under helium with low-pressure oxygen—Part 1: Sintered α-SiC

L. Charpentier [a,b], M. Balat-Pichelin [a,*], F. Audubert [b]

[a] *PROMES-CNRS, 7 rue du four solaire, 66120 Font-Romeu – Odeillo, France*
[b] *CEA, DEN/DEC/SPUA/LTEC, Cadarache, 13108 St Paul lez Durance, France*

Abstract

Gas-cooled Fast Reactor (GFR) is one system of the Generation IV International Forum systems studied by CEA (France). The considered coolant, helium, is pressurized at 7 MPa and the nominal working temperature is about 1300 K. In case of accident, reactor temperatures can reach 1900–2300 K. Several studies are carried out to determine the physico-chemical behavior of structural and cladding materials undergoing various environmental constraints. The cladding materials currently considered are refractory carbides, and particularly silicon carbide, SiC. Experimental tests at high temperature (1400–2100 K) on massive α-SiC samples coupled to mass variation, SEM and roughness analyses enabled to determine the transition between passive and active oxidation regimes, and to study the resistance to corrosion of such material in some conditions encountered in case of accident (high temperature increase up to 2300 K). The transition between passive and active oxidation obtained experimentally appears at 1300 K for an oxygen partial pressure of 0.2 Pa and at 1600 K for 100 Pa. The experimental mass loss rate obtained for conditions encountered during an accident – active oxidation – have shown that a maximal oxygen partial pressure of 10 Pa in helium is well suited to avoid a huge degradation of the α-SiC.

Keywords: Surfaces; Corrosion; SiC; Nuclear applications; High temperature

1. Introduction

Nuclear energy enables to satisfy the growth of the demand for electricity without affecting the fuel reserves and the climate through global warming and greenhouse effect. Therefore, there is a huge interest in increasing the efficiency of fission energy by producing energy at higher temperatures. This implies the conception of new nuclear systems. Ten countries have agreed on a framework for international research cooperation for a future generation of nuclear energy systems, known as Generation IV International Forum (GIF), using liquid sodium, molten salts or gaseous helium coolants instead of pressurized water. The conception of such reactors requires different safety and reliability issues than the current ones. One of particular interest is the GFR (Gas-cooled Fast Reactor) system, which features a fast-spectrum helium-coolant reactor and a closed fuel cycle. The nominal condition of use of this system is about 1300 K, with an elevated total pressure (7 MPa). Such high temperatures enable not only to deliver electricity, but also heat for different industrial processes (hydrogen production, reduction of metallic oxides, etc.) with high conversion efficiency. The main technological challenge is the development of materials resisting to damage at very high temperatures and fast-neutron fluences. Especially, SiC is an excellent candidate for these requirements.

This study focuses on the oxidation behavior of α-SiC under helium polluted with oxygen impurities (from 2 to 1000 ppm). The oxidation of silicon carbide obeys indeed to different mechanisms as a function of oxygen partial pressure and temperature:

(i) During passive oxidation (Eq. (1)), mainly at low temperature and high oxygen partial pressure, a silica protective layer is formed at the surface of SiC preventing it from further oxidation:

$$SiC_{(s)} + (3/2)O_{2(g)} = SiO_{2(s)} + CO_{(g)} \quad (1)$$

(ii) During active oxidation (Eq. (2)), essentially at high temperature and low oxygen partial pressure, $SiO_{(g)}$ is produced and, consequently, no protective silica layer appears

* Corresponding author. Tel.: +33 468 307 768; fax: +33 468 302 940.
E-mail address: marianne.balat@promes.cnrs.fr (M. Balat-Pichelin).

0955-2219/$ – see front matter © 2010 Elsevier Ltd. All rights reserved.
doi:10.1016/j.jeurceramsoc.2010.04.025

whereas SiC is characterized by significant mass loss:

$$SiC_{(s)} + O_{2(g)} = SiO_{(g)} + CO_{(g)} \quad (2)$$

Previous studies[1–5] refer to transitions from passive to active oxidation regime, theoretical or experimental, according to the partial pressure of oxygen and temperature, but not at the lower oxygen partial pressures encountered in this study. The discrepancy between the experimental results obtained for the position of the active to passive transition can be explained by different parameters: the polytype of the silicon carbide, its microstructure, its composition (impurities or sintering aid content), the gas flow, the partial and total pressures, the method used and the criterion taken to define the transition.[1]

The present study is done as in the literature there is hardly no experimental data on the active to passive transition under helium with oxygen partial pressure pO_2 and temperature ranges of interest for GFR applications (i.e. $pO_2 \leq 100$ Pa and $T \geq 1300$ K). It continues the works from Eck et al.[4] who performed a theoretical study for the determination of the passive to active transition and studied the oxidation behavior under a total pressure of 7×10^4 Pa of helium with different oxygen contents on both pressure-

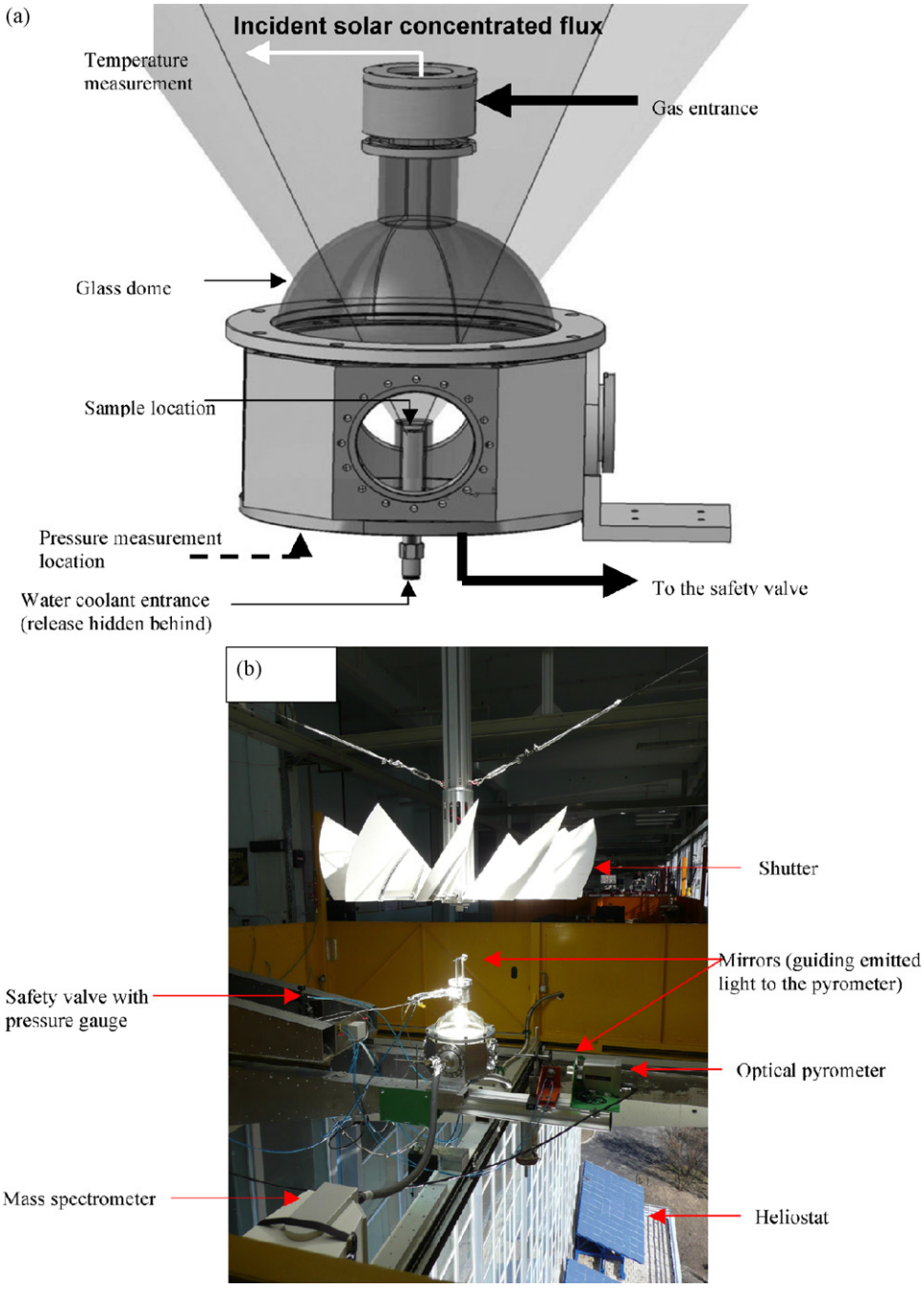

Fig. 1. Schematic representation (a) and image (b) of the REHPTS facility.

less sintered α-SiC and β-SiC produced by chemical vapor deposition.

2. Experimental procedure

In this work, we focused on the experimental determination of the transition between passive and active oxidation and also on the behavior in conditions encountered in case of accident for a α polytype, using the REHPTS (REacteur Hautes Pression et Température Solaire) facility and surface characterization through Scanning Electron Microscopy (SEM) and profilometry (mean square roughness RMS and maximal roughness variation R_{max} measurements).

2.1. Experimental set-up

The scheme and picture of the experimental set-up called REHPTS are presented in Fig. 1. A flat heliostat servo-controlled to the apparent movement of the sun is reflecting the incident solar flux to a spherical facetted concentrator. A shutter enables to control the fraction of the concentrated solar flux delivered, therefore the temperature of the sample placed inside the reactor. The device is composed of a stainless steel reactor with a cooled sample-holder and covered with a glass hemispherical top. It allows the heating of samples up to 2500 K thanks to the concentration of the solar radiation and the available total pressures (max 3×10^5 Pa) are limited by the mechanical resistance of the glass hemispherical top. This set-up is placed to have the sample located 25 mm above the focus of the solar furnace, thus elevated temperatures on materials such as SiC may be obtained at very fast rate (up to 100 K/s) on a homogeneous 10 mm diameter area. A monochromatic (5 μm) optical pyrometer and two mirrors allow to measure the surface temperature of the sample through a fluorine window. The spectral normal emissivity taken for SiC is 0.90 at this wavelength and it does not change during passive or active oxidation, silica presenting the same emissivity than SiC at this wavelength. The accuracy of the temperature measurements is going from 1400 ± 15 K to 2100 ± 22 K.

To reproduce the GFR atmosphere, different helium qualities from Air Liquide (He Alphagaz 1 quality with 2 ppm O_2, 1 ppm H_2O contents and He U quality with up to 20 ppm O_2 content) were used with a gas flow of 10 l min^{-1}. Pure oxygen (O_2 alphagaz N48 quality with 2 ppm H_2O and 6 ppm N_2) was added to helium U through a second gas line in order to increase the content of the O_2 impurity up to 1000 ppm. A safety valve with a gauge enabled us to work with a constant total pressure of 10^5 Pa under gas flow. Therefore the partial pressure of oxygen, pO_2 could vary between 0.2 and 100 Pa, according to the controlled oxygen content. The gas phase composition inside the reactor is checked by a mass spectrometer (©Pfeiffer Omnistar Vacuum GSD 301).

2.2. Materials and oxidation protocol

The silicon carbide studied is α-SiC from Boostec (France). It is processed by pressureless sintering around 2300 K with B_4C additive. The tested samples, squares of 20 mm side and 2 mm thickness, were polished using fine diamond powders before experiment to obtain a mean square roughness of 0.1 μm. The α-SiC samples present an excess of carbon, as revealed by the XPS analysis: the atomic ratio Si/C is nearly 0.85 on the surface after Ar^+ etching, much lower at the native contaminated surface.

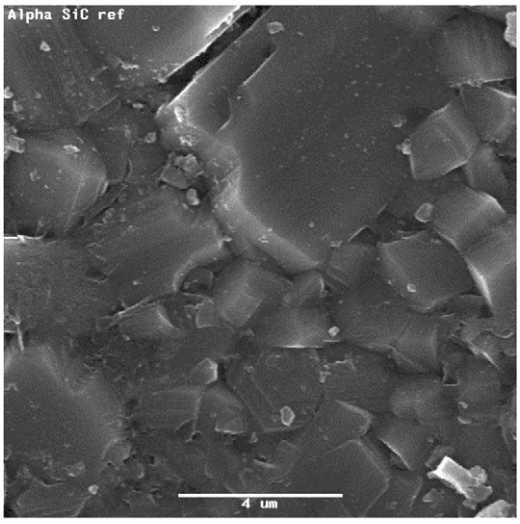

Fig. 2. SEM image of the surface of α-SiC sample before oxidation. The length of the scale bar is 4 μm.

The surface of the samples was analyzed with SEM before oxidation (Fig. 2). The average grain size of such samples, estimated from several SEM images, is comprised between 2.5 and 5 μm.

Samples were oxidized during 10 min at constant temperature inside the REHPTS. Fig. 3 presents an example of the temperature and pressure variations during one experiment. The heating rate up to the plateau is between 20 and 100 K s^{-1}. The rate of decrease from the plateau to the room temperature is also very fast (≈20 K s^{-1}). The total pressure inside the reactor quickly increases (resp. decreases) during the heating (resp. cooling) step and the total pressure slowly varies on the temperature plateau around $10^5 \pm 0.05 \times 10^5$ Pa. The gauge prevents the total pressure from increasing higher than this value.

The high heating and cooling rates present two advantages. The first one is that the order of magnitude is the same than the one of the rates expected in case of incident or accident in the GFR. The second one is that the steps of heating and cooling that do not exceed 1 min each are fast enough to prevent any reaction during these transient steps. Therefore a 10 min plateau is sufficient compared to the duration of transient steps to set that the oxidation mainly occurs during the plateau. For comparison, a thermogravimetric set-up heats and cools the sample at slower rates (>10 K min^{-1}), so it takes more than one hour to reach the desired temperature. So the plateau must exceed several hours and the oxidation during transient steps of heating and cooling cannot be neglected. Indeed, thermogravimetric analysis is a better tool for in situ kinetic analysis in determined conditions.[6]

Mass variations were measured by weighting the samples before and after oxidation, and were converted to rates of mass changes, expressed in mg cm^{-2} h^{-1}. SEM imaging and roughness measurement (one-dimensional profilometry, Hom-

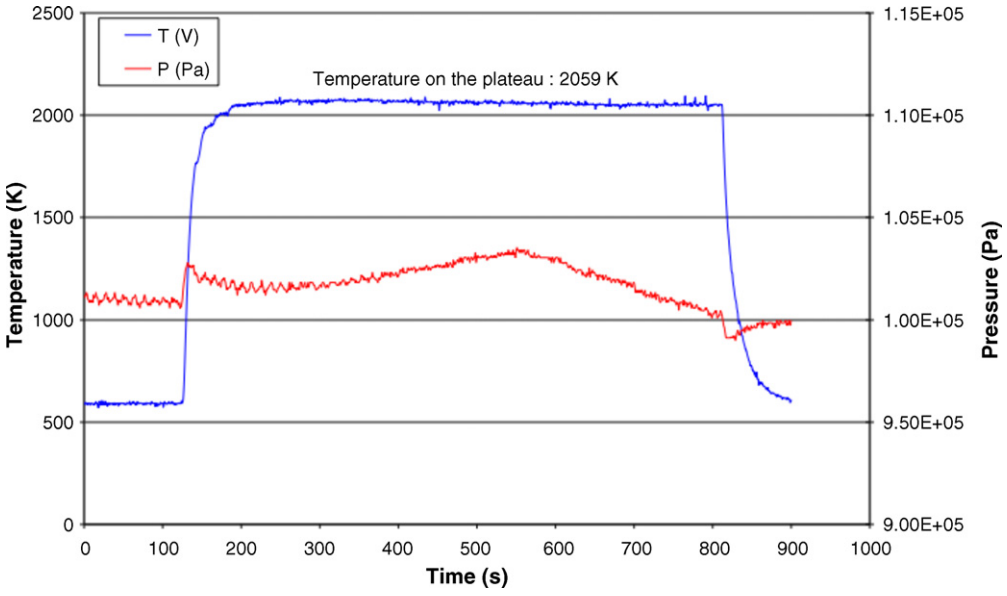

Fig. 3. Illustration of the temperature and pressure variations during one experiment (sample O).

mel Tester T2000) were performed to analyze the surface morphology of the samples before and after oxidation. The mean square roughness (RMS) and the maximal roughness variation (R_{max}) were measured along six 5 mm-long trajectories at different angles in order to estimate a pertinent average for each analyzed sample. Mass variations, SEM observations and roughness measurements enabled to determine the oxidation regime (passive or active).

3. Results and discussion

Table 1 presents the different experimental results obtained on the different tested samples according to the experimental conditions (T, pO_2). During all the experiments the total pressure was close to 10^5 Pa. A slight mass loss may be measured even in passive oxidation conditions due to the consumption of the excess carbon. We can notice in Table 1 that, in active oxidation conditions, the mass loss rate significantly increases with temperature whatever the partial pressure of oxygen. In this table, the temperature between passive and active oxidation can be obtained for each partial pressure of oxygen: for example, at $pO_2 = 2$ Pa, the transition temperature is around 1600 K; if the partial pressure increases up to 100 Pa, then the transition temperature is close to 1640 K.

Table 1
Relative mass variation, mass loss rates and oxidation regime for α-SiC according to temperature T and oxygen partial pressure pO_2.

α-SiC sample	pO_2 (Pa)	T (K)	Oxidation regime	$\Delta m/m$ (%)	Mass variation rate (mg cm^{-2} h^{-1})
T	0.2	1553	Passive	−0.022	−0.75
S	0.2	1600	Active	−0.028	−1.00
V	0.2	1900	Active	−0.235	−8.72
W	0.2	1925	Active	−0.477	−16.02
K	2	1407	Passive	+0.017	+0.58
I	2	1532	Passive	+0.004	+0.15
L	2	1602	Passive	0	0
B	2	1730	Active	−0.024	−0.90
C	2	1880	Active	−0.172	−5.83
D	2	2078	Active	−0.479	−19.01
N	10	1604	Passive	−0.008	−0.28
J	10	1680	Active	−0.016	−0.61
G	10	1716	Active	−0.067	−2.45
R	10	1917	Active	−0.236	−8.20
F	100	1637	Passive	−0.008	−0.32
M	100	1762	Active	−0.259	−9.24
H	100	1800	Active	−0.355	−12.65
O	100	2059	Active	−0.666	−23.38

SEM images enable to determine the oxidation regime close to the transition under $pO_2 = 0.2$ Pa (Fig. 4), 2 Pa (Fig. 5) and 100 Pa (Fig. 6), in addition of mass variations if they are not significant enough to differentiate active from passive regimes. In these figures, we observe in the (a) images the presence of a silica layer, characteristic of the passive regime, and in the (b) images the presence of damaged surface with grain etching, characteristic of the active one. The higher the partial pressure is the more significant the differences are. The (c) images are obtained on samples tested under conditions that can be encountered during an accident respectively at 1900 K (sample V, Fig. 4), 2078 K (sample D, Fig. 5) and 2059 K (sample O, Fig. 6). We can notice in Figs. 5(c) and 6(c) that at higher temperatures, the grains look bigger than on the reference (Fig. 2), this can be due to the removal of the smaller grains by active oxidation, and/or to the grains growth.

Table 2 presents the measurements of the mean square roughness RMS and of the maximal roughness variation R_{max} for the reference sample and for some oxidized samples under $pO_2 = 0.2$, 2 and 100 Pa, at various temperatures. We can notice that the passively oxidized sample presents RMS and R_{max} values very close to the one of the reference sample, whereas the actively oxidized samples are rougher close to the transition. The RMS and R_{max} values of actively oxidized samples above

Table 2
Mean square roughness RMS and maximum roughness variation R_{max} (using 1D-profilometry) measured for reference α-SiC and oxidized samples under various pO_2.

Sample (temperature and oxidation regime)	Reference α-SiC	T (1553 K, passive)	S (1600 K, active)	V (1900 K, active)
$pO_2 = 0.2$ Pa				
RMS (μm)	0.116	0.120	0.188	0.262
R_{max} (μm)	1.042	0.905	1.628	2.558
Sample (temperature and oxidation regime)	Reference α-SiC	L (1602 K, passive)	B (1730 K, active)	D (2078 K, active)
$pO_2 = 2$ Pa				
RMS (μm)	0.116	0.113	0.172	0.128
R_{max} (μm)	1.042	0.980	2.362	1.225
Sample (temperature and oxidation regime)	Reference α-SiC	F (1637 K, passive)	M (1762 K, active)	O (2059 K, active)
$pO_2 = 100$ Pa				
RMS (μm)	0.116	0.117	0.218	0.212
R_{max} (μm)	1.042	0.863	1.892	1.698

2000 K (samples D and O) are lower than the ones of actively oxidized samples at temperatures closer to the transition (samples B and M). As shown in Figs. 4–6, the silica formation on SiC under passive regime smoothens the surface of the sample, whereas the etching of the grains under active regime sharpens it, excepted at very high temperature (Figs. 5(c) and 6(c)) where grains growth occurs. So 1D-profilometry is also a quick characterization tool to determine the location of the transition, but at very high temperatures ($T > 2000$ K), the important mean size of the grains may involve a decrease of the roughness compared to actively oxidized samples closer to the transition.

Fig. 7 reports the theoretical[4] – full line – and the experimental passive to active transition – dotted line – in the oxidation of α-SiC with the experimental data. In Fig. 7 are also plotted the experiments carried out on the α-SiC samples: the black squares correspond to the samples that are in the domain of passive oxidation, with a protective layer on the surface, and the open squares are for the samples that underwent active oxidation. The experimental transition marked by the dotted line is plotted at the limit of the samples under passive oxidation for safety margins. Experimental Arrhenius law was determined according to these conditions and compared to the theoretical transition we calculated in a former study,[4] using thermodynamic calculations with the software GEMINI[7] and the Wagner modified model.[1,8] Table 3 reports the theoretical and experimentally determined transition temperatures according to pO_2 for α-SiC. We can notice that the experimental transition is higher than the theoretical one under very low pO_2, but the difference is decreasing while pO_2 is increasing, from 260 K under $pO_2 = 0.2$ Pa to 40 K under $pO_2 = 100$ Pa. The activation energy and pre-exponential coefficient are therefore much higher for experimental law ($E_a = 1540$ kJ/mol; $A = 7 \times 10^{50}$ Pa) than for the theoretical one ($E_a = 360$ kJ/mol; $A = 5 \times 10^{13}$ Pa). This difference between theory and experience can be explained mainly by the kinetic barriers that may favor the stability of silica at higher temperature than expected from thermodynamic calculations.

Table 3
Transition temperatures T^{p-a} calculated[4] and experimentally determined for α-SiC according to the oxygen partial pressure pO_2.

pO_2 (Pa)	Theoretical T^{p-a} (K)[4]	Experimental T^{p-a} (K)
0.2	1300	1560
2	1400	1600
10	1470	1610
100	1600	1640

In order to simulate and analyze the effects of conditions encountered during an accident, oxidation was studied at temperatures far from the transition up to 2100 K. Fig. 8 presents the evolution of the mass loss rates according to temperature and oxygen partial pressure. Fig. 8 gives a clear vision of the impact of temperature on the mass loss rate. It increases with temperature following a linear trend up to 2100 K. These linear trends (and the temperature range they have been determined) are the following ones (with corresponding correlation coefficient):

Under $pO_2 = 0.2$ Pa, $v = 0.0376T - 59.399$ ($R^2 = 0.82$)
for $1600 \leq T \leq 1925$ K

Under $pO_2 = 2$ Pa, $v = 0.0528T - 91.499$ ($R^2 = 0.97$)
for $1730 \leq T \leq 2100$ K

Under $pO_2 = 10$ Pa, $v = 0.0309T - 50.902$ ($R^2 = 0.99$)
for $1680 \leq T \leq 1920$ K

Under $pO_2 = 100$ Pa, $v = 0.053T - 84.685$ ($R^2 = 0.97$)
for $1630 \leq T \leq 2100$ K

We can notice in Fig. 8 and Table 1 that for $pO_2 = 100$ Pa, the mass loss rate is much more important than under $pO_2 \leq 10$ Pa,

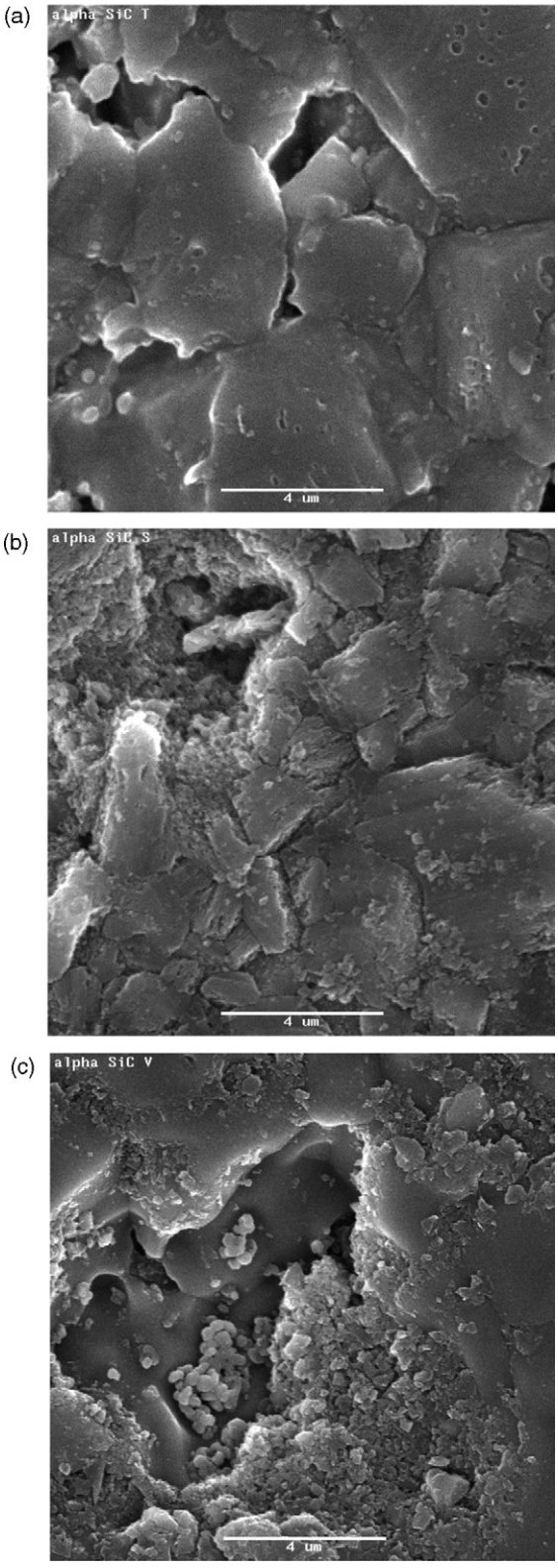

Fig. 4. SEM images of α-SiC oxidized under $pO_2 = 0.2$ Pa and at (a) $T = 1553$ K (sample T); (b) $T = 1600$ K (sample S); (c) $T = 1900$ K (sample V). The length of the scale bar is 4 μm.

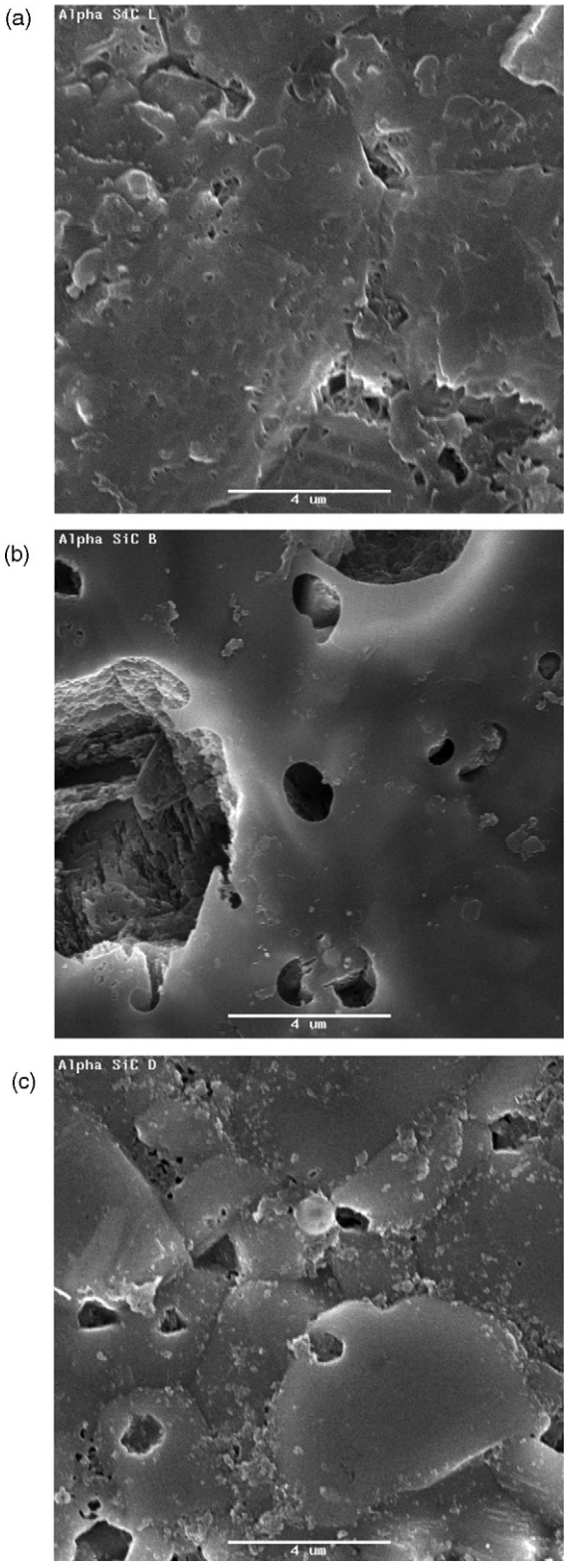

Fig. 5. SEM images of α-SiC oxidized under $pO_2 = 2$ Pa and at (a) $T = 1602$ K (sample L); (b) $T = 1730$ K (sample B); (c) $T = 2078$ K (sample D). The length of the scale bar is 4 μm.

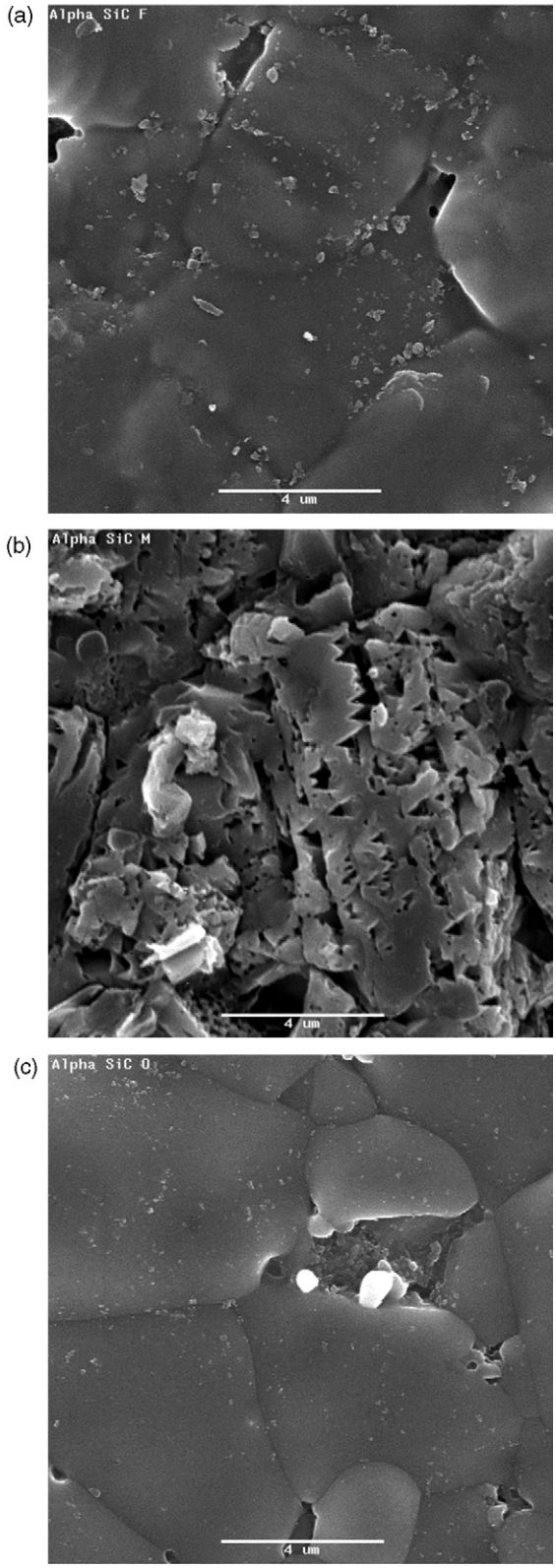

Fig. 6. SEM images of α-SiC oxidized under $pO_2 = 100$ Pa and at (a) $T = 1637$ K (sample F); (b) $T = 1762$ K (sample M); (c) $T = 2059$ K (sample O). The length of the scale bar is 4 μm.

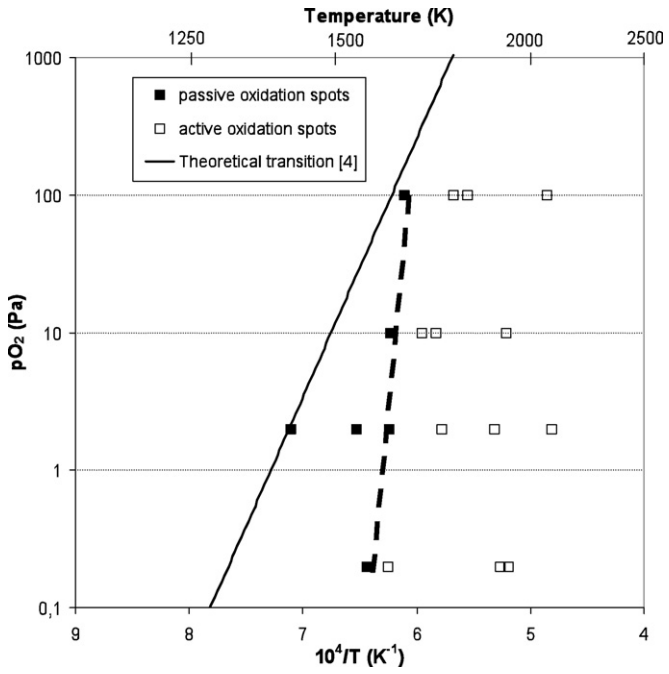

Fig. 7. Theoretical (full line) and experimental (dotted line) transition from passive to active oxidation for α-SiC using an Arrhenius plot. The points represent the performed experiments (black squares: samples under passive oxidation, open squares: samples under active oxidation).

for temperatures higher than 1700 K, and increases with temperature up to 23 mg cm^{-2} h^{-1} at 2060 K. The effect of increasing the oxygen partial pressure on the active oxidation kinetics of SiC was already mentioned and explained in by several authors, among them Hinze,[3] Gulbransen[9] and Narushima.[10] The mass loss increase with oxygen partial pressure is due to the fact that the reaction rate is controlled by the oxygen diffusion in the boundary layer interface.

For the application aimed, increasing pO_2 above 10 Pa in the helium coolant may lead to more important damages of the materials under conditions encountered in case of accident in the GFR reactor.

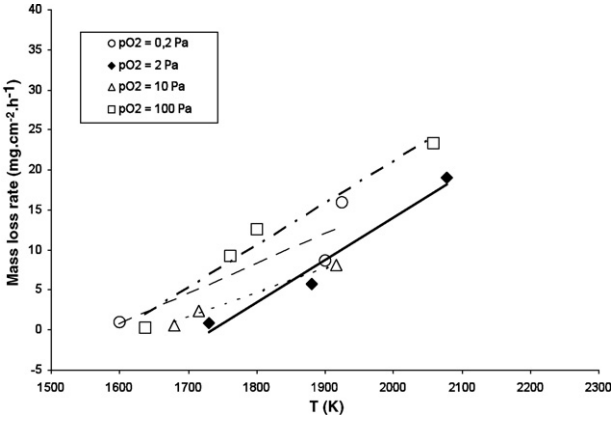

Fig. 8. Mass loss rates (in mg cm^{-2} h^{-1}) of α-SiC versus temperature in active conditions for various pO_2.

4. Conclusion

This study was done to understand the behavior of α-SiC under helium with oxygen partial pressure and temperature ranges of interest for GFR applications. We have determined the experimental transition law (Arrhenius fit) between passive and active oxidation regime for oxygen partial pressure from 0.2 to 100 Pa, under a helium total pressure of 10^5 Pa, and studied the variations of α-SiC mass loss rates according to the temperature and the oxygen partial pressure under conditions that might be encountered in case of accident ($T > 1500$ K).

We noticed that an increase of pO_2 have two consequences:

- the positive effect for the aimed application is to report the transition temperature up to higher temperatures far from the nominal working conditions (1300 K) of the GFR,
- the negative effect is to increase the α-SiC damage under conditions that can be representative of an accident (for temperature up to 2300 K). This effect is especially significant for $pO_2 = 100$ Pa.

For α-SiC used as cladding material in the GFR, a very high purity helium is therefore not required to insure a good compromise: a pO_2 of 2–10 Pa is sufficient to enable the passive oxidation regime under nominal conditions without having too significant mass losses under conditions encountered during an accident.

This study will be continued on the oxidation behavior of another polytype of SiC, β-SiC obtained by Chemical Vapor Deposition CVD, in order to investigate the impact of the crystallographic structure (hexagonal or cubic) of the SiC on the transition between active and passive oxidation and on the evolution of the mass loss rates at very high temperatures up to 2300 K.

Acknowledgements

The authors thank the research groups MATINEX and GEDEPEON for their financial support and CEA for the funding of the post-doctoral position of L. Charpentier.

References

1. Balat MJH. Determination of the active-to-passive transition in the oxidation of silicon carbide in standard and microwave-excited air. *J Eur Ceram Soc* 1996;**16**:55–62.
2. Vaughn WL, Maahs HG. Active-to-passive transition in the oxidation of silicon carbide and silicon nitride in air. *J Am Ceram Soc* 1990;**73**:1540–3.
3. Hinze JW, Graham HC. The active oxidation of silicon and silicon carbide in the viscous gas flow regime. *J Electrochem Soc* 1976;**123**:1066–73.
4. Eck J, Balat-Pichelin M, Charpentier L, Bêche E, Audubert F. Behavior of SiC at high temperature under helium with low oxygen partial pressure. *J Eur Ceram Soc* 2008;**28**:2995–3004.
5. Ogura Y, Morimoto T. Mass spectrometric study of oxidation of SiC in low-pressure oxygen. *J Electrochem Soc* 2002;**149**:J47–52.
6. Charpentier L, Maître A, Balat-Pichelin M, Foucaud S, Audubert F. Influence of alumina on the passive oxidation at low oxygen pressure of hot-pressed α-SiC. *Scr Mater* 2009;**60**:481–4.
7. *Thermodata*, 6 rue du tour de l'eau, 38400 Saint Martin d'Hères, France.
8. Wagner C. Passivity during the oxidation of silicon at elevated temperature. *J Appl Phys* 1958;**29**:1295–7.
9. Gulbransen EA, Andrew KF, Brassart FA. The oxidation of silicon carbide at 1150° to 1400 °C and at 9×10^{-3} to 5×10^{-1} Torr oxygen pressure. *J Electrochem Soc* 1966;**113**:1311–4.
10. Narushima T, Goto T, Iguchi Y, Hirai T. High-temperature active oxidation of chemically vapor-deposited silicon carbide in an Ar–O_2 atmosphere. *J Am Ceram Soc* 1991;**74**:2583–6.